Short-Range Correlations and the EMC Effect in Effective Field Theory

Jiunn-Wei Chen, William Detmold, Joel E. Lynn, and Achim Schwenk

Phys. Rev. Lett. **119**, 262502 — Published 29 December 2017

DOI: 10.1103/PhysRevLett.119.262502

Short Range Correlations and the EMC Effect in Effective Field Theory

Jiunn-Wei Chen,[1,2,*] William Detmold,[2,†] Joel E. Lynn,[3,4,‡] and Achim Schwenk[3,4,5,§]

[1] *Department of Physics, CTS and LeCosPA, National Taiwan University, Taipei 10617, Taiwan*
[2] *Center for Theoretical Physics, Massachusetts Institute of Technology, Cambridge, MA 02139, USA*
[3] *Institut für Kernphysik, Technische Universität Darmstadt, 64289 Darmstadt, Germany*
[4] *ExtreMe Matter Institute EMMI, GSI Helmholtzzentrum für Schwerionenforschung GmbH, 64291 Darmstadt, Germany*
[5] *Max-Planck-Institut für Kernphysik, Saupfercheckweg 1, 69117 Heidelberg, Germany*

We show that the empirical linear relation between the magnitude of the EMC effect in deep inelastic scattering on nuclei and the short range correlation scaling factor a_2 extracted from high-energy quasi-elastic scattering at $x \geq 1$ is a natural consequence of scale separation and derive the relationship using effective field theory. While the scaling factor a_2 is a ratio of nuclear matrix elements that individually depend on the calculational scheme, we show that the ratio is independent of this choice. We perform Green's function Monte Carlo calculations with both chiral and Argonne-Urbana potentials to verify this and determine the scaling factors for light nuclei. The resulting values for ^{3}He and ^{4}He are in good agreement with experimental values. We also present results for ^{9}Be and ^{12}C extracted from variational Monte Carlo calculations.

Introduction: Deep Inelastic Scattering (DIS) of leptons on hadrons can be precisely described as high-energy (perturbative) lepton-quark scattering weighted by the parton distribution functions (PDFs) that describe the probability of finding a quark or gluon inside the hadron. DIS has been used to map out the quark and gluon parton distributions for the proton and subsequently nuclei. In recent years, these experiments have revealed new and intriguing glimpses of nuclear structure that we seek to derive using effective field theory (EFT) methods.

In 1983, the European Muon Collaboration [1] measured the structure functions $F_2^A(x, Q^2)$ describing DIS for iron and deuterium targets, where Bjorken $x = Q^2/(2p\cdot q)$ and $Q^2 = -q^2$ are defined in terms of the target four-momentum p and the momentum transfer from the lepton to the target, q. The results of these experiments could not be explained by nuclear structure (i.e., momentum distribution of nucleons inside the nucleus) without modifying the nucleon structure [1]. This "EMC effect" was unexpected since the typical binding energy per nucleon is so much smaller (<1%) than the nucleon mass and the energy transfer involved in a DIS process. The EMC effect has now been mapped out for DIS on targets ranging from helium to lead (see Refs. [2–6] for reviews) and similar medium modifications of parton structure have been investigated in other reactions [5, 7]. The picture that has emerged is that the ratio

$$R_{\rm EMC}(A,x) = \frac{2F_2^A(x,Q^2)}{AF_2^d(x,Q^2)}, \tag{1}$$

with A the atomic number and d the deuteron, can deviate from unity by up to 20% over the range $0.05 < x < 0.7$. The ratio has very little dependence on Q^2 and so we suppress it. Experimental data also suggest that for an isoscalar nucleus, the x and A dependence of $R_{\rm EMC} - 1$ is factorizable. That is, the shape of the deviation of $R_{\rm EMC}$ from unity is independent of A while the magnitude of the deviation depends only on A [8, 9]. $R_{\rm EMC}$ forms a straight line in intermediate x, and one can express the magnitude of the EMC effect by the slope $dR_{\rm EMC}(A,x)/dx$ for $0.35 \leq x \leq 0.7$. Since Bjorken x is defined with respect to the parent nucleon of the struck parton, it is bounded in the range $0 \leq x \leq A$.

In recent experiments at Jefferson Lab, it was found that the ratio of quasi-elastic (QE) scattering cross sections,

$$a_2(A,x) \equiv \left.\frac{2\sigma_A}{A\sigma_d}\right|_{1.5<x<2}, \tag{2}$$

forms an x-independent plateau with negligible Q^2 dependence for targets from ^{3}He to ^{197}Au [10–14]. This factor a_2 is referred to as the short range correlation (SRC) scaling factor. A remarkable empirical discovery is that the EMC slope and the SRC scaling factor a_2 are linearly related [15, 16].

In this Letter, we explain this linear relationship using EFT and compute a_2 in light nuclei. We first review the EFT description of the EMC effect of Ref. [17] which explained the factorization of x and A dependence of $R_{\rm EMC} - 1$, and then show that the linear relation follows naturally from this. Factorization also shows that, up to higher order corrections, a_2 is scheme and scale independent even though it arises from scheme- and scale-dependent matrix elements in different nuclei. Finally, the values of a_2 for ^{3}He and ^{4}He are computed using the Green's function Monte Carlo (GFMC) method with both chiral and Argonne-Urbana potentials to confirm the scheme and scale independence and are compared with data, showing close agreement. Results for ^{9}Be and ^{12}C extracted from variational Monte Carlo (VMC) calculations [18] are also discussed.

EFT Analysis: Chiral EFT is constructed based on the chiral symmetry of QCD. It has been successfully applied to many aspects of meson [19], single [20], and multi-nucleon systems [21]. In particular, chiral EFT has been applied to PDFs in the meson and single-nucleon

[22–27] and multi-nucleon sectors [17, 28] as well as to other light-cone dominated observables [29–33].

The structure functions describing lepton-nucleus DIS, $F_2^A(x,Q^2)$, can be expressed in terms of nuclear PDFs $q_i^A(x,Q)$ (for simplicity of presentation, we choose the DIS scheme where the renormalization and factorization scale are set equal to the hard scale of DIS, $\mu=\mu_f=Q$, although the results below do not depend on the scheme) as $F_2^A(x,Q^2)=\sum_i Q_i^2 x\, q_i^A(x,Q)$, where the sum is over quarks and anti-quarks of flavor i of charge $\pm Q_i$ in a nucleus A. In what follows, we focus on the isoscalar PDFs, $q^A=q_u^A+q_d^A$; in the relevant experiments, nuclear PDFs are typically "corrected" for isospin asymmetry of the targets. The dominant (leading-twist) parton distributions are determined by target matrix elements of bilocal light-cone operators. Applying the operator product expansion, the Mellin moments of the parton distributions,

$$\langle x^n\rangle_A(Q)=\int_{-A}^{A} x^n q_A(x,Q)dx, \tag{3}$$

are determined by matrix elements of local operators,

$$\langle A;p|\mathcal{O}^{\mu_0\cdots\mu_n}|A;p\rangle=\langle x^n\rangle_A(Q)\,p^{(\mu_0}\dots p^{\mu_n)} \tag{4}$$

with

$$\mathcal{O}^{\mu_0\cdots\mu_n}=\overline{q}\gamma^{(\mu_0}iD^{\mu_1}\cdots iD^{\mu_n)}q, \tag{5}$$

where (...) indicates that enclosed indices have been symmetrized and made traceless and $D^\mu=(\overrightarrow{D}^\mu-\overleftarrow{D}^\mu)/2$ is the covariant derivative.

In nuclear matrix elements of these operators, there are other relevant momentum scales below Q: $\Lambda\sim 0.5$ GeV is the range of validity of the EFT, and $P\sim m_\pi$ is a typical momentum inside the nucleus (m_π is the pion mass). These scales satisfy $Q\gg\Lambda\gg P$ and the ratio Λ/Q is the small expansion parameter in the twist expansion while the ratio $\epsilon\sim P/\Lambda\sim 0.2-0.3$ is the small expansion parameter for the chiral expansion.

In EFT, each of the QCD operators is matched to hadronic operators at scale Λ [17]

$$\begin{aligned}\mathcal{O}^{\mu_0\cdots\mu_n}\to&:\langle x^n\rangle_N M^n v^{(\mu_0}\cdots v^{\mu_n)}N^\dagger N\left[1+\alpha_n N^\dagger N\right],\\&+\langle x^n\rangle_\pi \pi^\alpha i\partial^{(\mu_0}\cdots i\partial^{\mu_n)}\pi^\alpha+\dots:,\end{aligned} \tag{6}$$

where the operators enclosed by : : are normal ordered (with respect to the vacuum state), N (π) is the nucleon (pion) field, v is the nucleon four velocity and $\langle x^n\rangle_{N(\pi)}$ is the nth moment of the isoscalar quark PDF in a free nucleon (pion). The $\langle x^n\rangle_{N\,(\pi)}$ terms are one-body operators acting on a single hadron only, while the α_n terms are two-body operators. Here we have only kept the SU(4) (spin and isospin) singlet two-body operator $\propto\left(N^\dagger N\right)^2$ and neglected the SU(4) non-singlet operator $\propto(N^\dagger\boldsymbol{\sigma}N)^2-(N^\dagger\boldsymbol{\tau}N)^2$ which changes sign when interchanging the spin ($\boldsymbol{\sigma}$) and isospin ($\boldsymbol{\tau}$) matrices [34]. The latter operator has an additional $O(1/N_c^2)\sim 0.1$ suppression in its prefactor [35] with N_c the number of colors. We also replace the nucleon velocity by the nucleus velocity and include the correction $i\partial/M$ to higher orders.

The relative importance of the hadronic operators of Eq. (6) in a nuclear matrix element can be systematically estimated from the power counting of the EFT, which assigns a power of the small expansion parameter ϵ to each Feynman diagram. In Weinberg's power counting scheme [36], the nucleon one-body operator is $\mathcal{O}(\epsilon^{-3})$, the nucleon two-body operator is $\mathcal{O}(\epsilon^0)$, while the pion one-body operator connecting two nucleons is $\mathcal{O}(\epsilon^{n-1})$. Since $\langle x^n\rangle_\pi=0$ for even n due to charge conjugation symmetry, the $n=1$ pion operator enters at $\mathcal{O}(\epsilon^0)$ but for higher n the contributions either vanish or are higher order compared with the other operators in Eq. (6).

The same order of importance for these operators is also found using the alternate power countings of Refs. [37–39], but with a less suppressed two-body effect compared with the one-body nucleon operator. Other higher dimensional operators are omitted here because they are higher order in the power counting [17].

Using nucleon number conservation, $\langle A|:N^\dagger N:|A\rangle=A$, the nuclear matrix element of Eq. (6) for $n\neq 1$ is

$$\langle x^n\rangle_A(Q)=\langle x^n\rangle_N(Q)\Big[A+\alpha_n(\Lambda,Q)\langle A|:(N^\dagger N)^2:|A\rangle_\Lambda\Big], \tag{7}$$

where α_n is A independent but Λ dependent and is completely determined by the two-nucleon system. After an inverse Mellin transform, the isoscalar PDFs satisfy

$$q_A(x,Q)/A\simeq q_N(x,Q)+g_2(A,\Lambda)\tilde{q}_2(x,Q,\Lambda), \tag{8}$$

where

$$g_2(A,\Lambda)=\frac{1}{2A}\big\langle A|:(N^\dagger N)^2:|A\big\rangle_\Lambda, \tag{9}$$

and $\tilde{q}_2(x,Q,\Lambda)$ is an unknown function independent of A.[1] This result also holds at the level of the structure function [17],

$$F_2^A(x,Q^2)/A\simeq F_2^N(x,Q^2)+g_2(A,\Lambda)f_2(x,Q^2,\Lambda). \tag{10}$$

The second term on the right-hand side of Eq. (10) is the nuclear modification of the nucleon structure function F_2^N. The shape of distortion, i.e., the x dependence of f_2, which is due to physics above the scale Λ, is A independent and hence universal among nuclei. The magnitude of distortion, g_2, which is due to physics below the scale Λ, depends only on A and Λ.

Linear EMC-SRC relation in EFT: At smaller Q^2, we can generalize the analysis in the previous section to

[1] The exception of $n=1$ in Eq. (7) results from the relevant contribution of the pionic operator in that case. This implies that factorization is violated only for $x=0$ [40].

all higher twist terms in the operator product expansion. For a higher twist operator $\mathcal{O}^{\mu_0\cdots\mu_n}$, its indexes need not to be symmetric nor traceless, but the matching is still similar to Eq.(6). The only difference is that chiral symmetry dictates that the pion one-body operator has at least two derivatives in the chiral limit even if the operator has no index. For example, twist-three operators $G^2_{\alpha\beta}$ and $m_q\bar{q}q$ are matched to $(\partial\pi)^2$ and $m_\pi^2\pi^2$ operators. Therefore the same power counting result holds to all orders in the twist expansion and we have

$$\sigma_A/A \simeq \sigma_N + g_2(A,\Lambda)\sigma_2(\Lambda), \tag{11}$$

where the E (initial electron energy), x and Q^2 dependence of σ_i is suppressed.

With σ_N vanishing for $x > 1$, Eqs. (2) and (11) imply

$$a_2(A, x > 1) \simeq \frac{g_2(A,\Lambda)}{g_2(2,\Lambda)}, \tag{12}$$

for both DIS and QE kinematics yielding a plateau in a_2 as observed experimentally at $1.5 < x < 2$. (Fermi motion, an $\mathcal{O}(\epsilon)$ effect in the EFT, extends the contribution of the single nucleon PDF to x slightly above 1 so the onset of the plateau is also pushed to larger x.) Since $a_2(A,x)$ is a ratio of physical quantities, it is independent of the EFT cutoff scale Λ. The EFT analysis also predicts that the scale dependence of $g_2(A,\Lambda)$ is independent of A as suggested in [41].

From Eqs. (1) and (10), direct computation shows the that

$$\frac{dR_{\mathrm{EMC}}(A,x)}{dx} \simeq C(x)\,[a_2(A) - 1] \tag{13}$$

has a linear relation with a_2, with $C(x) = g_2(2)[f_2' F_2^N - f_2 F_2^{N'}]/[F_2^N + g_2(2) f_2]^2$ independent of A and Λ (here, $f' = df/dx$).

SRC scaling factor: Short-range correlations in light nuclei have been examined theoretically from several points of view [18, 42–47]. However, the focus of previous studies was on the one- or two-body distribution functions in coordinate or momentum space, which are scale and scheme dependent [48, 49].

Here we discuss their observable ratio, the SRC scaling factor, Eq. (12). We calculate a_2 using the GFMC method, which is one of the most accurate methods for solving the many-body Schrödinger equation for nuclei up to $A \le 12$ [50]. The GFMC method projects out the lowest-energy state of a given Hamiltonian H from a trial wave function $|\Psi_T\rangle$ via the many-body imaginary-time Green's function

$$\lim_{\tau\to\infty} e^{-H\tau}\,|\Psi_T\rangle \to |\Psi_0\rangle\,, \tag{14}$$

with τ the imaginary time and $|\Psi_0\rangle$ the exact many-body ground state. A limitation of diffusion Monte Carlo methods is that they require local potentials in practice,

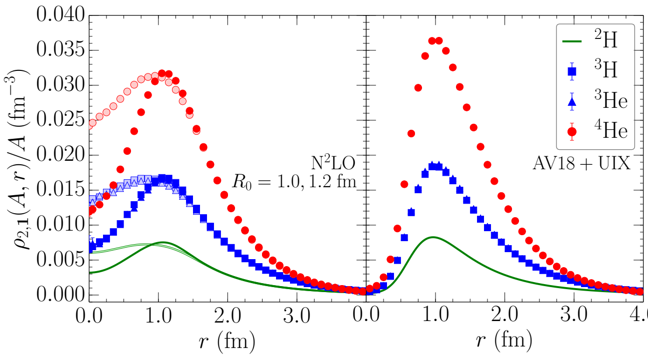

FIG. 1. Scaled two-body distribution function $\rho_{2,\mathbf{1}}(A,r)/A$ for $A = 2,3,4$ nuclei as a function of relative separation r for chiral interactions at N^{2}LO with two different cutoffs (left panel) and for the AV18+UIX potentials (right panel). In the left panel, the darker (lighter) points are for $R_0 = 1.0$ fm ($R_0 = 1.2$ fm). $A = 2$ is solved exactly. For $A = 3,4$ the error bars visible at small r are GFMC statistical uncertainties. The variation of the short-distance behavior of the distributions shows clearly their scale and scheme dependence.

while nuclear forces derived from chiral EFT are usually nonlocal. Recently local chiral EFT interactions have been derived up to next-to-next-leading order (N^{2}LO) in Weinberg power counting [51–55]. This enables us to use the GFMC method with chiral EFT as well as phenomenological interactions to study the scale and scheme independence of a_2.

The function $g_2(A,\Lambda)$ of Eq. (9) can be obtained from the isoscalar two-body distribution

$$\rho_{2,\mathbf{1}}(A,r) = \frac{1}{4\pi r^2}\Big\langle \Psi_0 \Big| \sum_{i<j}^{A} \delta(r - |\mathbf{r}_i - \mathbf{r}_j|) \Big| \Psi_0 \Big\rangle, \tag{15}$$

as a matrix element of a local operator,

$$g_2(A,\Lambda) = \rho_{2,\mathbf{1}}(A, r=0)/A. \tag{16}$$

In Eq. (15), $\mathbf{r}_i$ is the position of the ith nucleon and the sum runs over all pairs in the nucleus, so that the integral over $\rho_{2,\mathbf{1}}(A,r)$ is normalized to $A(A-1)/2$. We note that our EFT approach is not based on the experimentally observed np-pair dominance [57, 58], but instead on the fact that, of the two S-wave two-nucleon operators, the SU(4)-symmetric operator, $(N^\dagger N)^2$ (counting all pairs) is dominant over the SU(4)-nonsymmetric operator (suppressed by a factor $\mathcal{O}(1/N_c^2) \sim 0.1$). Thus, we include all pairs in Eq. (15). Nevertheless, at short internucleon separations, we find a predominance of np pairs over pp pairs by a factor $\sim$ 5–10 for ^{4}He and ^{12}C. In our GFMC calculations, the two-body distribution function is obtained from a mixed estimate; for details see Ref. [59].

Figure 1 shows the scaled two-body distribution function $\rho_{2,\mathbf{1}}(A,r)/A$ for $A = 2,3,4$ nuclei for chiral two- and

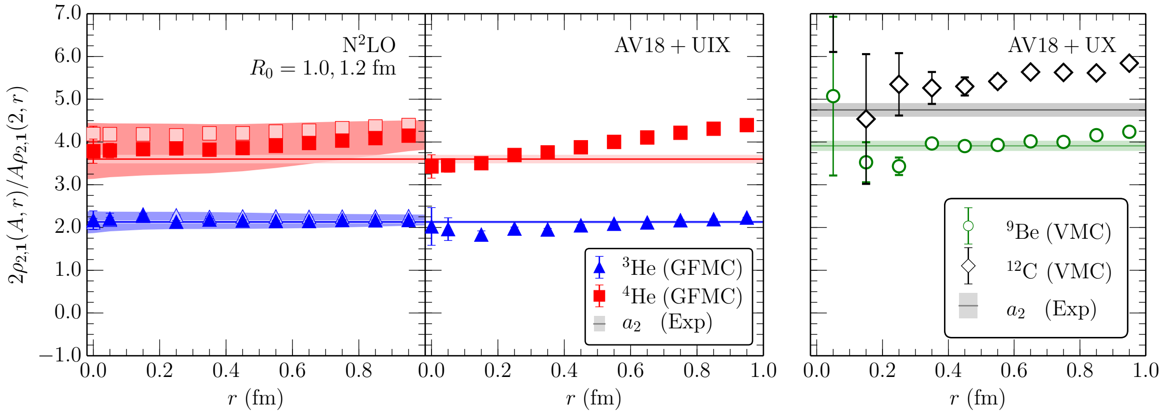

FIG. 2. Ratio of the two-body distribution functions for ^{3}He (blue) and ^{4}He (red) to the two-body distribution function for the deuteron, $2\rho_{2,\mathbf{1}}(A,r)/A\rho_{2,\mathbf{1}}(2,r)$, as a function of relative separation r. Results are shown for chiral interactions at N^{2}LO with two different cutoffs (left panel) and for the AV18+UIX potentials (middle panel) calculated using the GFMC method. In the left panel, the darker (lighter) points are for $R_0 = 1.0$ fm ($R_0 = 1.2$ fm) and the bands represent a combined uncertainty estimate from the truncation of the chiral expansion added in quadrature to the GFMC statistical uncertainties. The right panel shows the ratio for ^{9}Be (green) and ^{12}C (black) for AV18+UX obtained from VMC results [56]. These ratios are compared to the experimental values for a_2 from Ref. [16], given by the horizontal lines.

three-nucleon interactions at N^{2}LO as well as for the phenomenological Argonne v_{18} (AV18) two-nucleon [60] plus the UIX three-nucleon [61] potentials. The varying behavior of the two-body distributions at small separation r makes clear that $g_2(A,\Lambda)$ depends both on the scheme and scale, where the latter is especially clear from the cutoff dependence ($R_0 = 1.0$ fm vs. $R_0 = 1.2$ fm). Analogous to PDFs, one- and two-body distribution functions depend on the renormalization scheme and scale and hence are not physical quantities [49]. However, the factorization derived in EFT shows the ratio a_2 should be scheme and scale independent.

Using Eqs. (12) and (16), a_2 is obtained from the ratio

$$a_2 \simeq \lim_{r\to 0} \frac{2\,\rho_{2,\mathbf{1}}(A,r)}{A\,\rho_{2,\mathbf{1}}(2,r)}, \tag{17}$$

where we calculate the behavior at $r = 0$ by linearly extrapolating from the smallest two r values to zero separation. In EFT, locality only means a shorter distance than the resolution scale. Hence, we expect one can replace $r \to 0$ in Eq. (17) by smearing within $r < R$ (a scale set by, but not necessarily equal to, R_0), and still get the same a_2.

We see indeed this is the case in Fig. 2. The left two panels show a_2 for ^{3}He and ^{4}He calculated using the GFMC method with the chiral N^{2}LO interactions and for the phenomenological AV18+UIX potentials. The right panel shows results extracted from VMC calculations [56] for the AV18+UX potentials for ^{9}Be and ^{12}C. The red and blue bands in the left panel represent a combined uncertainty estimate from the truncation of the chiral expansion [62] added in quadrature to the GFMC statistical uncertainties. The $\mathcal{O}(\epsilon^2) \sim 0.1$ corrections to the

TABLE I. Results for the SRC scaling factor a_2 obtained via Eq. (17) from GFMC calculations of $A = 2,3,4$ nuclei based on chiral N^{2}LO interactions (for cutoffs $R_0 = 1.0$ and 1.2 fm) and the AV18+UIX potentials. The uncertainties quoted for the N^{2}LO interactions include the uncertainty estimated from the truncation of the chiral expansion added in quadrature to the GFMC statistical uncertainties.

	N^{2}LO ($R_0 = 1.0 - 1.2$ fm)	AV18+UIX	Exp. [16]
^{3}H	2.1(2) – 2.3(3)	2.0(4)	
^{3}He	2.1(2) – 2.1(3)	2.0(4)	2.13(4)
^{4}He	3.8(7) – 4.2(8)	3.4(3)	3.60(10)

operator are also contained within this conservative uncertainty estimate. We display the band obtained for the $R_0 = 1.0$ fm cutoff which encompasses the N^{2}LO calculations with both cutoffs ($R_0 = 1.0, 1.2$ fm). For each panel, it is clear that a plateau in the ratio sets in at a value R depending on the scale and scheme. Moreover, we observe from Fig. 2 that the $r = 0$ value is a conservative estimate for a_2 given that the statistical uncertainties in the calculation of the two-body distributions grow as we approach zero separation. As is evident from Fig. 2, the GFMC values for a_2 are in very good agreement with experiment [16] while the preliminary VMC results are also encouraging. We summarize the extracted SRC scaling factors a_2 of the GFMC calculations and the comparison with experiment in Table I.

Summary and outlook: We have shown that the linear relation between the magnitude of the EMC effect at intermediate x and the SRC scaling factor a_2 is a natural consequence of scale separation and have derived this result using EFT. We have also computed a_2 for ^{3}He and ^{4}He using the GFMC method with both chiral and Argonne-Urbana potentials to confirm the scheme and scale independence.

GFMC calculations with chiral interactions for ^{9}Be, ^{12}C and other light nuclei will allow further tests of the EFT understanding of these phenomena. In the case of ^{9}Be, it would be especially interesting to confirm whether a_2 is determined by local instead of global nuclear density [63]. It would also be very insightful to complete our theoretical understanding of the EMC-SRC relation by computing the $C(x)$ coefficient in Eq. (13) from lattice QCD calculations of $f_2(x)$ from the deuteron [64–66].

The EFT approach to the partonic structure of nuclei has broader applicability than to the isoscalar structure that we have discussed above. For the $F_3(x, Q^2)$ structure function that is accessible in weak-current DIS, EFT predicts a relation analogous to Eq. (10) with F_2 replaced by F_3, and g_2 replaced by an isospin-dependent nuclear matrix element. The resulting analogue of Eq. (13) is also expected to hold. The generalization to spin-dependent parton structure and to generalized parton distributions [67] is similarly straight forward. EFT could also shed light on whether a plateau of $\sigma_A/\sigma_{^3\mathrm{He}}$ for $2 < x < 3$ exists, which is still inconclusive experimentally [10, 14, 68].

Acknowledgments: We thank Or Hen, Evgeny Epelbaum, Dick Furnstahl, Martin Hoferichter, Dean Lee, Ulf-G. Meißner, Jerry Miller, and Akaki Rusetsky for useful comments and discussions. This work was supported in part by MOST of Taiwan under Grant Nos. 102-2112-M-002-013-MY3 and 105-2918-I-002-003, DOE Early Career Research Award DE-SC0010495, DOE Grant No. DE-SC0011090, the ERC Grant No. 307986 STRONGINT, the MIT MISTI program and the Kenda Foundation of Taiwan. The computations were performed at NERSC, which is supported by the US Department of Energy under Contract No. DE-AC02-05CH11231, and on the Lichtenberg high performance computer of the TU Darmstadt.

* jwc@phys.ntu.edu.tw
† wdetmold@mit.edu
‡ joel.lynn@gmail.com
§ schwenk@physik.tu-darmstadt.de

[1] J. J. Aubert *et al.* (European Muon Collaboration), Phys. Lett. B **123**, 275 (1983).
[2] M. Arneodo, Phys. Rept. **240**, 301 (1994).
[3] D. F. Geesaman, K. Saito, and A. W. Thomas, Annu. Rev. Nucl. Part. Sci. **45**, 337 (1995).
[4] G. Piller and W. Weise, Phys. Rept. **330**, 1 (2000).
[5] P. R. Norton, Rept. Prog. Phys. **66**, 1253 (2003).
[6] O. Hen, D. W. Higinbotham, G. A. Miller, E. Piasetzky, and L. B. Weinstein, Int. J. Mod. Phys. E **22**, 1330017 (2013).
[7] J. C. Peng, P. L. McGaughey, and J. M. Moss, in *RIKEN Symposium and Workshop on Selected Topics in Nuclear Collective Excitations (NUCOLEX 99) Wako, Japan, March 20-24, 1999* (1999) hep-ph/9905447.
[8] S. Daté, K. Saito, H. Sumiyoshi, and H. Tezuka, Phys. Rev. Lett. **52**, 2344 (1984).
[9] L. L. Frankfurt and M. I. Strikman, Phys. Rept. **160**, 235 (1988); Phys. Rept. **76**, 215 (1981).
[10] N. Fomin, J. Arrington, R. Asaturyan, F. Benmokhtar, W. Boeglin, P. Bosted, A. Bruell, M. H. S. Bukhari, M. E. Christy, E. Chudakov, *et al.*, Phys. Rev. Lett. **108**, 092502 (2012).
[11] O. Hen, E. Piasetzky, and L. B. Weinstein, Phys. Rev. **C85**, 047301 (2012), arXiv:1202.3452 [nucl-ex].
[12] L. L. Frankfurt, M. I. Strikman, D. B. Day, and M. Sargsian, Phys. Rev. **C48**, 2451 (1993).
[13] K. S. Egiyan *et al.* (CLAS), Phys. Rev. **C68**, 014313 (2003), arXiv:nucl-ex/0301008 [nucl-ex].
[14] K. S. Egiyan *et al.* (CLAS Collaboration), Phys. Rev. Lett. **96**, 082501 (2006).
[15] L. B. Weinstein, E. Piasetzky, D. W. Higinbotham, J. Gomez, O. Hen, and R. Shneor, Phys. Rev. Lett. **106**, 052301 (2011).
[16] O. Hen, E. Piasetzky, and L. B. Weinstein, Phys. Rev. C **85**, 047301 (2012).
[17] J.-W. Chen and W. Detmold, Phys. Lett. B **625**, 165 (2005).
[18] R. B. Wiringa, R. Schiavilla, S. C. Pieper, and J. Carlson, Phys. Rev. C **89**, 024305 (2014).
[19] J. Gasser and H. Leutwyler, Annals Phys. **158**, 142 (1984).
[20] V. Bernard, N. Kaiser, and U.-G. Meissner, Int. J. Mod. Phys. E **4**, 193 (1995).
[21] S. R. Beane, P. F. Bedaque, W. C. Haxton, D. R. Phillips, and M. J. Savage, "From hadrons to nuclei: Crossing the border," in *At The Frontier of Particle Physics* (World Scientific, 2012) Chap. 11, pp. 133–269; S. R. Beane, P. F. Bedaque, M. J. Savage, and U. van Kolck, Nucl. Phys. A **700**, 377 (2002); P. F. Bedaque and U. van Kolck, Ann. Rev. Nucl. Part. Sci. **52**, 339 (2002); K. Kubodera and T.-S. Park, Ann. Rev. Nucl. Part. Sci. **54**, 19 (2004); E. Epelbaum, H.-W. Hammer, and U.-G. Meißner, Rev. Mod. Phys. **81**, 1773 (2009); H.-W. Hammer, A. Nogga, and A. Schwenk, Rev. Mod. Phys. **85**, 197 (2013).
[22] D. Arndt and M. J. Savage, Nucl. Phys. A **697**, 429 (2002).
[23] J.-W. Chen and X. Ji, Phys. Lett. **B523**, 107 (2001); Phys. Rev. Lett. **87**, 152002 (2001).
[24] W. Detmold, W. Melnitchouk, J. W. Negele, D. B. Renner, and A. W. Thomas, Phys. Rev. Lett. **87**, 172001 (2001); W. Detmold, W. Melnitchouk, and A. W. Thomas, Phys. Rev. D **66**, 054501 (2002); Phys. Rev. D **68**, 034025 (2003).
[25] W. Detmold and C.-J. D. Lin, Phys. Rev. D **71**, 054510 (2005).
[26] P. Hägler *et al.* (LHPC Collaboration), Phys. Rev. D **77**, 094502 (2008).
[27] M. Göckeler *et al.* (QCDSF Collaboration), Phys. Rev. Lett. **92**, 042002 (2004).
[28] S. R. Beane and M. J. Savage, Nucl. Phys. A **761**, 259 (2005).
[29] J.-W. Chen and X. Ji, Phys. Rev. Lett. **88**, 052003 (2002); A. V. Belitsky and X. Ji, Phys. Lett. B **538**, 289 (2002).
[30] J.-W. Chen and I. W. Stewart, Phys. Rev. Lett. **92**,

202001 (2004).
[31] J.-W. Chen, W. Detmold, and B. Smigielski, Phys. Rev. D **75**, 074003 (2007).
[32] S.-i. Ando, J.-W. Chen, and C.-W. Kao, Phys. Rev. D **74**, 094013 (2006).
[33] M. Diehl, A. Manashov, and A. Schäfer, Eur. Phys. J. A **29**, 315 (2006).
[34] T. Mehen, I. W. Stewart, and M. B. Wise, Phys. Rev. Lett. **83**, 931 (1999).
[35] D. B. Kaplan and M. J. Savage, Phys. Lett. B **365**, 244 (1996).
[36] T.-S. Park, D.-P. Min, and M. Rho, Nucl. Phys. A **596**, 515 (1996).
[37] D. B. Kaplan, M. J. Savage, and M. B. Wise, Phys. Lett. B **424**, 390 (1998).
[38] D. B. Kaplan, M. J. Savage, and M. B. Wise, Nucl. Phys. B **534**, 329 (1998).
[39] M. Pavón Valderrama and D. R. Phillips, Phys. Rev. Lett. **114**, 082502 (2015), arXiv:1407.0437 [nucl-th].
[40] See Supplemental Material which includes Refs. [69–72] .
[41] R. J. Furnstahl, in *Proceedings, International Conference on Nuclear Theory in the Supercomputing Era (NTSE-2013)* (2013) p. 371, arXiv:1309.5771 [nucl-th].
[42] H. Feldmeier, W. Horiuchi, T. Neff, and Y. Suzuki, Phys. Rev. C **84**, 054003 (2011).
[43] A. Rios, A. Polls, and W. H. Dickhoff, Phys. Rev. C **89**, 044303 (2014).
[44] C. Ciofi degli Atti, Phys. Rept. **590**, 1 (2015).
[45] R. Weiss, B. Bazak, and N. Barnea, Phys. Rev. C **92**, 054311 (2015).
[46] J. Ryckebusch, W. Cosyn, and M. Vanhalst, J. Phys. **G42**, 055104 (2015), arXiv:1405.3814 [nucl-th].
[47] S. K. Bogner and D. Roscher, Phys. Rev. **C86**, 064304 (2012), arXiv:1208.1734 [nucl-th].
[48] R. J. Furnstahl and H. W. Hammer, Phys. Lett. B **531**, 203 (2002).
[49] R. J. Furnstahl and A. Schwenk, J. Phys. G **37**, 064005 (2010).
[50] J. Carlson, S. Gandolfi, F. Pederiva, S. C. Pieper, R. Schiavilla, K. E. Schmidt, and R. B. Wiringa, Rev. Mod. Phys. **87**, 1067 (2015).
[51] A. Gezerlis, I. Tews, E. Epelbaum, S. Gandolfi, K. Hebeler, A. Nogga, and A. Schwenk, Phys. Rev. Lett. **111**, 032501 (2013).
[52] J. E. Lynn, J. Carlson, E. Epelbaum, S. Gandolfi, A. Gezerlis, and A. Schwenk, Phys. Rev. Lett. **113**, 192501 (2014).
[53] A. Gezerlis, I. Tews, E. Epelbaum, M. Freunek, S. Gandolfi, K. Hebeler, A. Nogga, and A. Schwenk, Phys. Rev. C **90**, 054323 (2014).
[54] I. Tews, S. Gandolfi, A. Gezerlis, and A. Schwenk, Phys. Rev. C **93**, 024305 (2016).
[55] J. E. Lynn, I. Tews, J. Carlson, S. Gandolfi, A. Gezerlis, K. E. Schmidt, and A. Schwenk, Phys. Rev. Lett. **116**, 062501 (2016).
[56] "Two-nucleon densities," `https://www.phy.anl.gov/theory/research/density2/`, accessed: 2016-05-09.
[57] R. Subedi, R. Shneor, P. Monaghan, B. D. Anderson, K. Aniol, J. Annand, J. Arrington, H. Benaoum, F. Benmokhtar, W. Boeglin, *et al.*, Science **320**, 1476 (2008).
[58] O. Hen *et al.* (CLAS Collaboration), Science **346**, 614 (2014).
[59] B. S. Pudliner, V. R. Pandharipande, J. Carlson, S. C. Pieper, and R. B. Wiringa, Phys. Rev. C **56**, 1720 (1997).
[60] R. B. Wiringa, V. G. J. Stoks, and R. Schiavilla, Phys. Rev. C **51**, 38 (1995).
[61] S. C. Pieper, V. R. Pandharipande, R. B. Wiringa, and J. Carlson, Phys. Rev. C **64**, 014001 (2001).
[62] E. Epelbaum, H. Krebs, and U. G. Meißner, Eur. Phys. J. A **51**, 53 (2015).
[63] J. Seely, A. Daniel, D. Gaskell, J. Arrington, N. Fomin, P. Solvignon, R. Asaturyan, F. Benmokhtar, W. Boeglin, B. Boillat, *et al.*, Phys. Rev. Lett. **103**, 202301 (2009).
[64] W. Detmold, Phys. Rev. D **71**, 054506 (2005).
[65] X. Ji, Phys. Rev. Lett. **110**, 262002 (2013).
[66] H.-W. Lin, J.-W. Chen, S. D. Cohen, and X. Ji, Phys. Rev. D **91**, 054510 (2015).
[67] See, e.g., X. Ji, J. Phys. G **24**, 1181 (1998).
[68] D. W. Higinbotham and O. Hen, Phys. Rev. Lett. **114**, 169201 (2015).
[69] H. D. Politzer, Nucl. Phys. B **172**, 349 (1980).
[70] C. Arzt, Phys. Lett. B **342**, 189 (1995).
[71] B. L. Friman, V. R. Pandharipande, and R. B. Wiringa, Phys. Rev. Lett. **51**, 763 (1983).
[72] R. Schiavilla, R. B. Wiringa, S. C. Pieper, and J. Carlson, Phys. Rev. Lett. **98**, 132501 (2007).